Journal of Structural Geology, Vol. 9, No. 3, pp. 371 to 374, 1987
Printed in Great Britain

0191-8141/87 $03.00 + 0.00

Brevia

SHORT NOTES

Displacement efficiency of faults and fractures

W. G. HIGGS and G. D. WILLIAMS

Department of Geology, University College, P.O. Box 78, Cardiff CF1 1XL, U.K.

(*Received* 2 *April* 1986; *accepted in revised form* 7 *October* 1986)

Abstract—Faults and fractures evolve kinematically as Somigliana dislocations. As a result, displacement gradients are always present, with displacements reducing to zero at fault/fracture tips. We present a graphical method for the comparison of displacement gradients from fractures of various magnitudes and types. Displacement efficiency of a fault/fracture is defined as its ability to maximise displacement across its surface.

INTRODUCTION

INDIVIDUAL faults may be regarded as Somigliana dislocations (Eshelby 1973, King *et al.* 1973) in that they show a net slip or displacement that varies in magnitude continuously across a rupture surface. The areal extent of a rupture surface is limited by a dislocation loop or tip line where displacement dies to zero. Other geological features that may be regarded as Somigliana dislocations are intrusive dykes and sills which are tongue shaped bodies bounded by a tip marking the line of rupture of the country rock. Such an intrusion would grow by the radial migration of this rupture line. Displacement or offset of the wall rock can be measured by matching features across the intrusion. Fibre-filled tension gashes offer a unique example in which incremental displacement may be accurately measured along fibre trails (Durney & Ramsay 1973, Ramsay & Huber 1983).

In the case of a simple fault formed during one rupture event, the fault will initiate at a point (the hypocentre of a seismic fault) and the rupture surface will increase in area by the radial migration of the tip line. After the rupture event, the preserved displacement pattern would show a reducing displacement, possibly in a non-linear fashion, in all directions away from the point of fracture initiation, becoming zero at the tip line. A kinematic classification of this 'one-event' fault could be based on two parameters; fault length, measured in the slip direction, and maximum displacement. Normalised displacement magnitude (M_n) is given by:

$$M_n = d_{max}/l_{max} \quad (1)$$

where d_{max} is the maximum value of the net slip and l_{max} is the movement-parallel fault length. Using displacement magnitude, the 1906 San Francisco earthquake event can be classified as a strike–slip fault of $M_n = 1.4 \times 10^{-5}$ (net slip = 6 m, rupture surface length = 430 km) (Bullen & Bolt 1985).

The kinematic evolution of a fault rupture surface involves complex strain patterns notably in the region of the tip line. Several authors have recognised tip line folds associated with thrust faults (Elliott 1976, Hossack 1983, Suppe 1983, Williams & Chapman 1983). Using two-dimensional data from normal faults in Quaternary sediments in Japan, Muraoka & Kamata (1983) produced a theoretical model for displacement distribution on a circular rupture surface. More recently, Rippon (1985) has interpreted fault kinematics by contouring throw and hade on single fault planes from the Carboniferous Coal Measures of NE Derbyshire. King *et al.* (1973) recorded the evolution of a rupture surface using creepmetres on an active segment of an aseismic fault in California. They were able to record rates of displacement build-up and tip line propagation along the ground surface in one creep event.

Faults of various magnitudes, minor intrusions and tension gashes can yield information regarding gradients of displacements in two-dimensional cross sections, or in three dimensions if data from several sections are available (e.g. Rippon 1985). We shall now present a graphical method for the kinematic classification of fractures, utilising displacement gradients. This approach is based on the measurement of displacement magnitudes across fracture surfaces. All parameters are normalised to allow direct comparison between fractures of different types and scales.

NORMALISED DISPLACEMENT GRADIENTS

In a section parallel to the slip direction of a fault, displacement of markers can be directly measured to give net slip vectors. In an ideal, one-event fault, displacements (d) are measured at set distances (l) from the fault tip towards the point of initial rupture (Fig. 1). In order to standardise the technique, d and l are normalised by dividing each measure by its respective maximum

$$D_n = d/d_{max} \quad (2)$$
$$L_n = l/l_{max}. \quad (3)$$

In this way, the maximum fault length and maximum displacement become unity. A coordinate plot of normalised displacement (D_n) versus normalised fault length (L_n) yields a curve from (0, 0) at the fault tip to (1, 1) at the point of maximum displacement. The product of the curve gradient at any point and the normalised

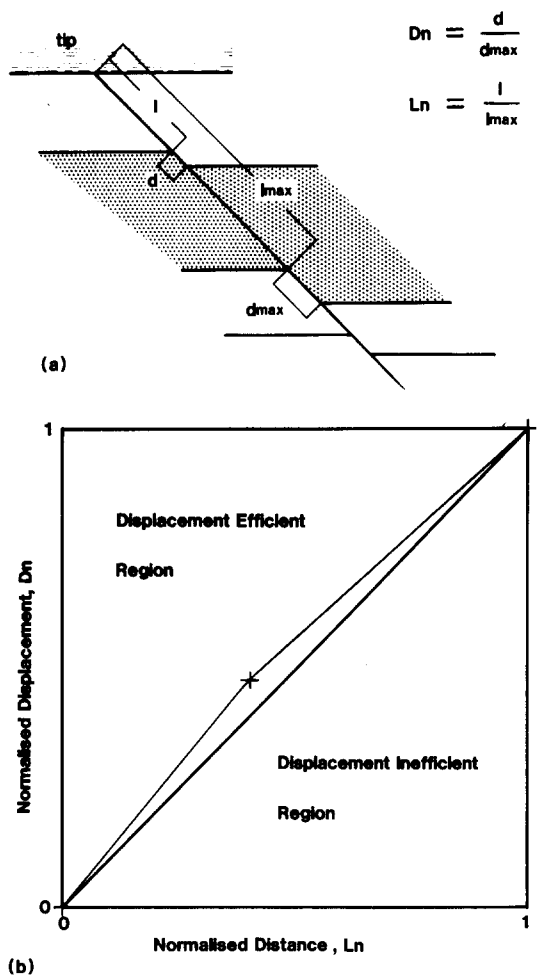

Fig. 1. (a) The upper portion of a normal fault in a cross section parallel to the net slip direction. Displacement of markers reduces upwards towards the fault tip. (b) Normalised displacement/distance plot.

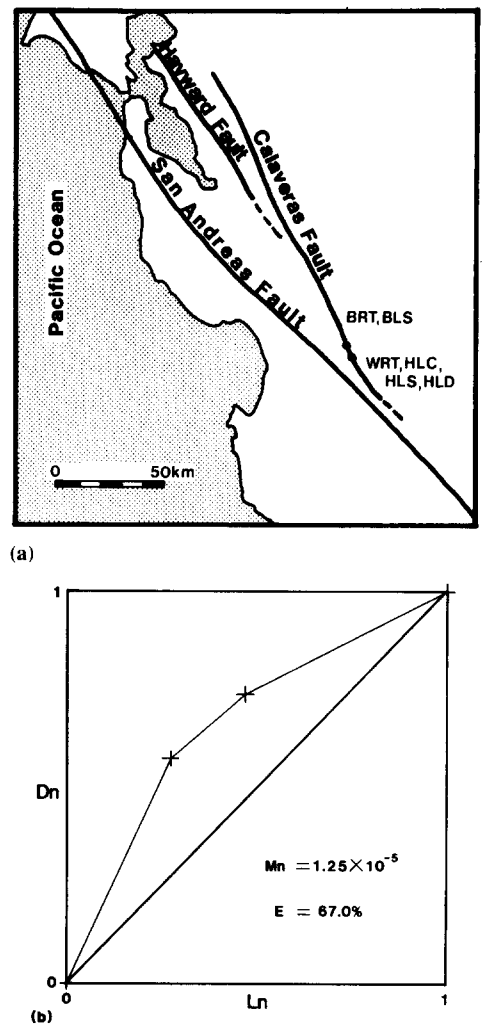

Fig. 2. (a) Map of the Calaveras fault showing the location of the aseismic creep event recorded by King *et al.* (1973). (b) Normalised displacement/distance plot of the Calaveras fault creep event. M_n = normalised displacement magnitude, E = displacement efficiency as a percentage.

displacement magnitude gives the fault displacement gradient (G) at that point:

$$G = M_n \cdot (\mathrm{d}D_n/\mathrm{d}L_n). \quad (4)$$

The area under the curve is a measure of displacement efficiency (E) of the fault. This is defined as the ability of the fault to maximise displacement over its surface, or in 2-D, over its length.

$$E = \int_0^1 f(L)\, \mathrm{d}D_n/\mathrm{d}L_n. \quad (5)$$

A fully slip-efficient fault would give a curve integral of 1 and this can be regarded as 100% displacement efficient. The curves produced for other faults/fractures may be compared with this 100% displacement efficient fault. An analogy for a highly displacement efficient fault is a crystallographic slip system, where the net slip of one lattice spacing exists over the whole slip surface; this slip reduces to zero in a very short distance at the dislocation loop. Faults such as this, that transmit maximum displacement over most of their area yield concave-down D_n/L_n graphs and high curve integrals approaching 1. The other end member of this continuum is a fault in which displacement falls off rapidly from its maximum value and records low displacements for the majority of its area or length. Such faults would give concave-up curves and low curve integrals approaching zero.

Using the Hayward–Calaveras fault (King *et al.* 1973) as an example (Fig. 2) the very low normalised displacement magnitude ($M_n = 2.8 \times 10^{-9}$) indicates a small slip transmitted over a very large rupture surface. The concave down nature of the curve and high curve integral ($E = 67\%$) indicates that this event was displacement efficient. The fault displacement data of Muraoka & Kamata (1983) suggest a mechanical control for the distribution of slip over fault surfaces (Fig. 3) as the D_n/L_n curve for a fault (Number 15) has two distinct regions. The curve from the point of maximum slip to the centre of the plot is markedly concave-down, indicating that the fault was displacement efficient in the region close to fault nucleation. However, from the centre of the plot to the fault tip the curve is concave-up suggesting that the fault became displacement inefficient towards the fault tip. The lithology through which the fault propagated exerted a mechanical control on the fault propagation/slip distribution. It appears that siltstones were better at maximising displacement than sandstones.

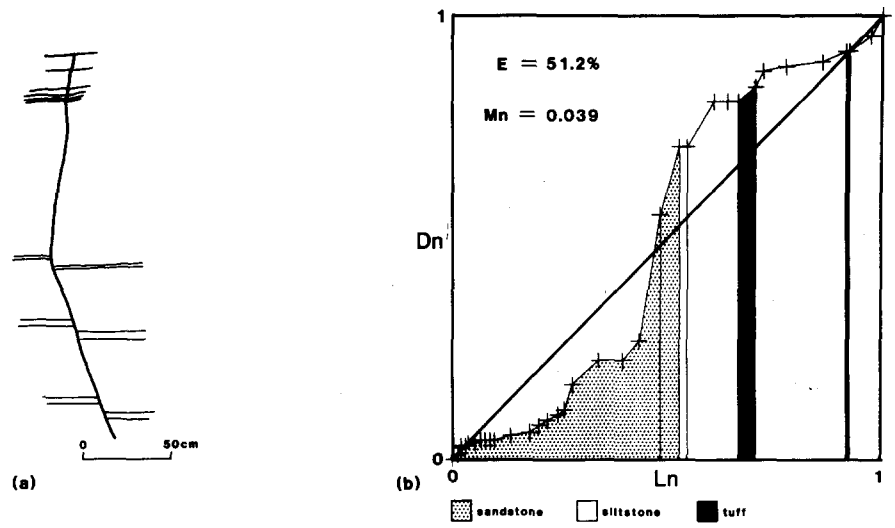

Fig. 3. (a) Movement-parallel section of fault 15 (after Muraoka & Kamata 1983) showing displaced markers. (b) Normalised displacement/distance plot of fault 15 in (a). The lithostratigraphy has been superimposed on the plot.

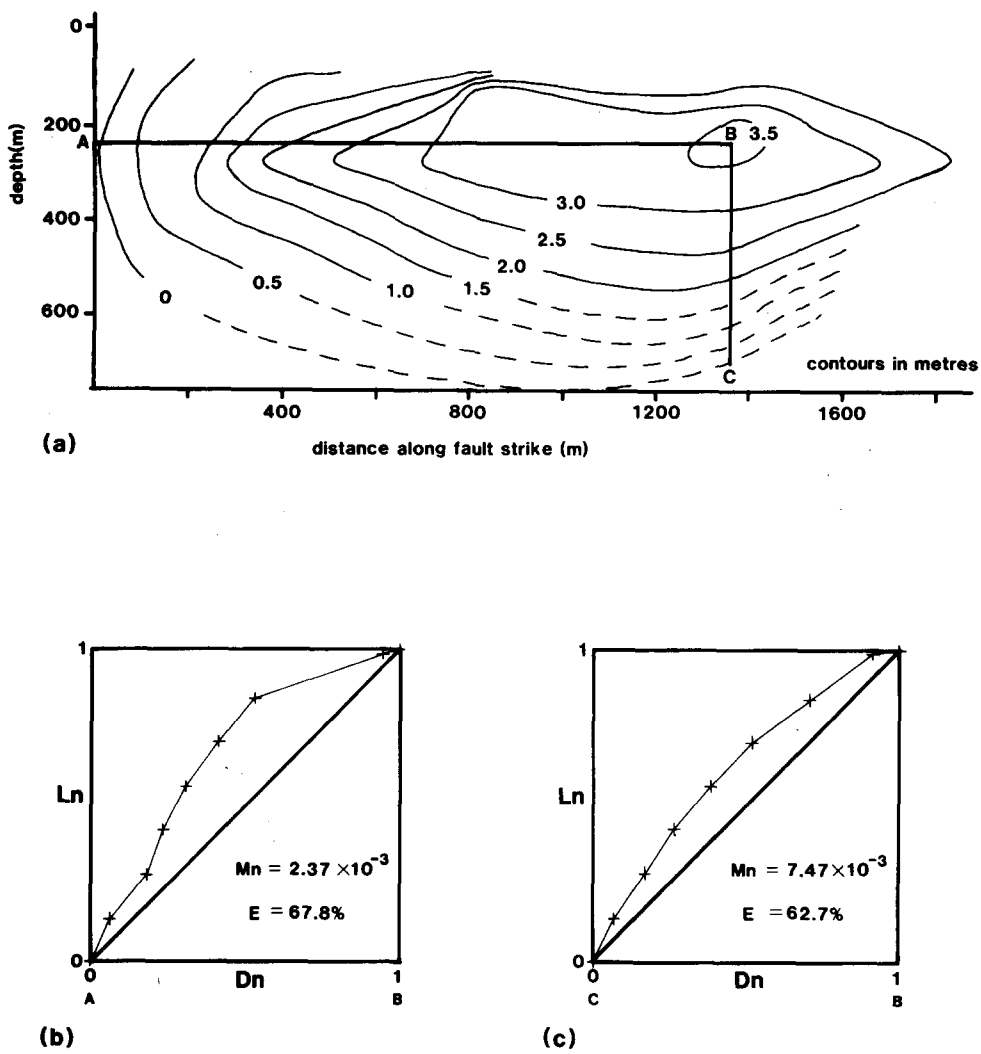

Fig. 4. (a) Contoured plot of dip separation (approximating to net slip) on a single fault plane from the coal measures of N Derbyshire (after Rippon 1985 fig. 4). (b) Normalised displacement/distance plot for section AB. (c) Normalised displacement/distance plot for section BC.

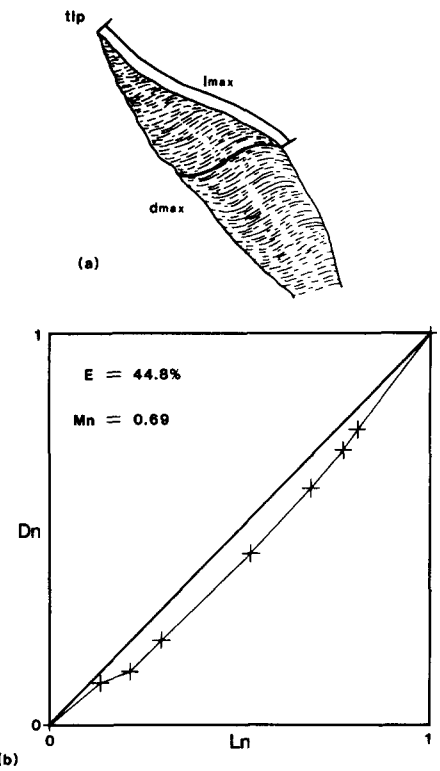

Fig. 5. (a) Tension gash containing curved calcite fibres that record the incremental opening history of the gash (after Ramsay & Huber 1983, fig. 13.5) *l*max = 2.4 mm. (b) Normalised displacement/distance plot for the upper part of the tension gash in (a).

A contoured plot of fault dip separation (Fig. 4) adapted from the work of Rippon (1985) may be used for three-dimensional analysis. Two plots (Figs. 4b & c) represent displacement distributions in sections along the fault surface: one parallel to fault strike and the other parallel to fault dip. Both plots show concave-down curves and high curve integrals suggesting that this fault is displacement efficient across its whole surface. A comparison of M_n values for the two sections of this fault relates directly to the greater fault width to length.

Curved calcite fibre trails in a tension gash (Fig. 5) record the incremental movement history of the opening of the gash (Durney & Ramsay 1973). It is possible to measure displacement along individual fibres which are distributed at various distances from the tension gash tip. A D_n/L_n plot indicates that the tension gash is displacement inefficient as the curve is concave up and its integral is low (E = 45%).

DISCUSSION

In a one-event fault, various displacement gradients may occur as a result of the relative variations in the rates of fault slip (S) and propagation (P) (cf. Williams & Chapman 1983). The ratio S/P is dimensionless and if it remained constant for the whole fault event, a straight line from origin to (1, 1) on the D_n/L_n plot would result. Any variation of the S/P ratio during the rupture event would give a non-linear plot such that when S/P is increasing a concave-down curve results, and when S/P is decreasing a concave-up one is produced. The former would be regarded as displacement efficient and the latter displacement inefficient. If we consider a fixed propagation rate, variations in displacement gradients may be considered in terms of slip rate only. A displacement efficient fault initiates with a low slip rate and slip rate progressively increases. A displacement inefficient fault initiates with a high slip rate which progressively decreases. The S/P ratio in a single-event fault is likely to be mechanically controlled and this may relate directly to lithological variations, to confining pressure or to pore fluid pressure. Also the geometry of faults will affect the fault efficiency; the efficiency of faults oriented in the direction of maximum critical resolved shear stress will differ from that of faults in other orientations.

The shape of the D_n/L_n curve provides a means of assessing the distribution of strain along the rupture surface. A 100% displacement efficient fault would require all of the strain due to rupture propagation to be taken up at the fault tip. However, a rupture of very low displacement efficiency would require only a small amount of strain to be accommodated at the fracture tip as a greater proportion would be distributed, possibly in a random manner, across the whole fault surface. Thus, displacement efficient faults have high tip strains whereas displacement inefficient faults distribute more strain across the whole fault surface. Strain concentration is represented by the steeper portions of the normalised displacement/distance curve. It is notable that all the faults and fractures presented here approximate to 50% displacement efficiency. If this observation is repeated, this may have important consequences in fault modelling and in the interpretation of faults in seismic sections, cross-sections and geological maps. Multiple event faults preserve the result of several overlapping dislocation movements with differing nucleation points, and the resulting curve may not be interpreted in this simple way but must be treated as a statistical sample of fault slip events.

REFERENCES

Bullen, K. E. & Bolt, B. A. 1985. *An Introduction to the Theory of Seismology*. Cambridge University Press.

Durney, D. W. & Ramsay, J. G. 1973. Incremental strains measured by incremental crystal growths. In: *Gravity and Tectonics* (edited by deJong, K. A. & Scholten, R.). Wiley, New York, 69–97.

Elliott, D. 1976. The energy balance and deformation mechanisms of thrust sheets. *Phil. Trans. R. Soc.* **A274**, 289–312.

Eshelby, J. D. 1973. Dislocation theory for geophysical application. *Phil. Trans. R. Soc.* **A274**, 331–338.

Hossack, J. R. 1983. A section through the Scandinavian Caledonides constructed with the aid of branch line maps. *J. Struct. Geol.* **5**, 103–111.

King, G. C. Y., Nason, R. D. & Tocher, D. 1973. Kinematics of fault creep. *Phil. Trans. R. Soc.* **A274**, 355–360.

Muraoka, H. & Kamata, H. 1983. Displacement distribution along minor fault traces. *J. Struct. Geol.* **5**, 483–495.

Ramsay, J. G. & Huber, M. I. 1983. *Techniques of Modern Structural Geology Vol. 1. Strain Analysis*. Academic Press, London.

Rippon, J. H. 1985. Contoured patterns of throw and hade of normal faults in the coal measures (Westphalian) of northeast Derbyshire. *Proc. Yorks. geol. Soc.* **45**, 147–161.

Suppe, J. 1983. Geometry and kinematics of fault bend folding. *Am. J. Sci.* **283**, 648–721.

Williams, G. D. & Chapman, T. J. 1983. Strains developed in the hangingwalls of thrusts due to their slip/propagation rates: a dislocation model. *J. Struct. Geol.* **5**, 563–571.